

# DEVELOPMENT OF CERIUM OXIDE-BASED INKJET INKS WITH LUSTRE EFFECT

**J. Manrique<sup>(1)</sup>, J. Usó<sup>(1)</sup>, F. Ferrando<sup>(1)</sup>, C. Rubert<sup>(1)</sup>, F.J. García-Ten<sup>(2)</sup>,  
M.J. Vicente<sup>(2)</sup>, A. Moreno<sup>(2)</sup>, R. Pérez<sup>(2)</sup>**

**(1) Ferro Spain, S.A.**

**(2) Instituto de Tecnología Cerámica (ITC). Asociación de Investigación de las  
Industrias Cerámicas (AICE). Universitat Jaume I. Castellón. Spain.**

## ABSTRACT

The materials being used for tile glazing and decoration in the ceramic sector are rapidly evolving owing to the swift, widespread implementation of inkjet printing technology. This has led to changes in traditional pigment inks and effect (lustre, white, metallised, etc.) inks, and glazes are currently being adapted to enable wholly digital (“full digital”) application.

A case in point is that of lustre-effect inks, which provide high gloss with tones that change according to the incident light, giving the tile a pearly appearance. This effect occurs when the incident light rays interact with a thin surface layer whose refractive index is much higher than that of the glaze coated by the ink.

Traditionally, this effect was obtained by reaction between certain glaze components (CaO) and a tungsten-contributing (W or WO<sub>3</sub>) raw material applied onto the glaze surface, which gave rise to a thin layer of scheelite (CaWO<sub>4</sub>) crystals, with a high refractive index (1.93) compared to that of the glass matrix (1.5). However, when glaze particle size is reduced for inkjet application, the glaze reaction surface area with the tungsten increases, a shell of CaWO<sub>4</sub> crystals being formed that surrounds that frit particles. The shell prevents viscous flow sintering of the glaze and leads to formation of a continuous surface layer of scheelite.

Another approach for obtaining the lustre effect with digital glazes involves using frits that devitrify cerium oxide and zirconium, with a high refractive index (2.15). This study addresses the development of inkjet inks with a lustre effect based on the aforementioned system, by analysing the different composition variables that affect the intensity of the sought-after lustre effect.

## 1. INTRODUCTION

The lustre or pearly effect stems from the way in which light interacts with objects when these have a thin surface layer whose refractive index differs from that of the substrate covered by this layer. In ceramic materials, such a surface layer can be obtained by different mechanisms: reaction between the underlying glaze frit and a material applied onto the surface of the unfired glaze composition [1][2], frit devitrification [3][4], precipitation of metallic particles at the glaze surface [5], and (chemical or physical) vapor phase deposition on a glazed tile.

The most widely used lustres in ceramic tile manufacturing are those based on scheelite (CaWO<sub>4</sub>) [1][2] and on cerium oxide and zirconium [3][4], hereafter referred to simply as cerium oxide, for the sake of brevity. In the scheelite-based lustres, during tile firing, an oriented surface layer of scheelite crystals forms owing to reaction of the calcium in the frit and tungsten, applied as an oxide or metal. Cerium lustres were later developed and the effect is due to the formation by devitrification at the glaze surface of a thin layer of oriented cerium oxide crystals [3][4].

The obtainment of glazed and decorated tiles entirely by inkjet technology (called "full digital") involves reducing the size of the jetted materials to below 3 µm. In previous studies it was verified that these conditions adversely affected obtainment of the scheelite-based lustre effect [6]. This is because the CaWO<sub>4</sub> formation mechanism is based on the sublimation of WO<sub>3</sub> applied from 750°C on and its subsequent reaction with the calcium in the frit particles at the surface. It was verified that when the frit had a d<sub>97</sub> of 40 µm, the reaction surface area was not very high and allowed a continuous surface layer of CaWO<sub>4</sub> to form, which produced the lustre effect. In contrast, when the frit particles were small (d<sub>97</sub>=3 µm), their reaction surface area increased, forming a skeleton of uniformly distributed CaWO<sub>4</sub> crystals, which covered the frit particles. The skeleton generated a rigid structure owing to the refractoriness of the CaWO<sub>4</sub> crystals, which prevented viscous flow sintering and, hence, formation of the surface film required for the sought-after decorative effect to materialise.

This study addresses the obtainment of the lustre effect by means of a frit that devitrifies cerium oxide and zirconium crystals, for use in production lines working with conventional glazes and in those that have incorporated full digital technology. To do so, the effect of particle size and composition of a lustre frit, as well as the influence of underlying glaze fusibility on the intensity of the lustre effect, was studied.

## 2. INFLUENCE OF FRIT PARTICLE SIZE

This section sets out the results obtained on modifying the particle size of a cerium oxide-devitrifying lustre frit. The frit was applied with a 40 g dry solids/m<sup>2</sup> laydown on a red-firing earthenware tile body, coated with a conventional transparent glaze, at two particle sizes,  $d_{97}=40\ \mu\text{m}$  (L-40) and  $d_{97}=3\ \mu\text{m}$  (L-3), and fired in a roller kiln at 1120°C. It was observed that frit L-40 provided a lustre effect, with a gloss value at 60° of 180, while frit L-3 did not yield said effect, so that the resulting gloss was similar to that of the underlying glaze (90).

In order to better understand why the effect pursued disappeared on reducing particle size, SEM observations were performed at each test sample surface and cross-section (Figure 1). Frit L-40 was observed to give rise to a surface coated with very small (150–250 nm) crystals (of a light colour in the image), which were responsible for the high gloss exhibited by the tile. These crystals formed a continuous layer at the surface and were embedded in the glass matrix, indicating that they had devitrified from the frit. Crystals were also observed at greater depth, though these were randomly distributed, probably at what had initially been the frit particle edges. The small size of the crystals prevented their chemical composition from being accurately determined. X-ray diffraction tests were therefore performed, which detected cerium oxide as main crystalline phase.

The appearance of the tile applied with the frit milled to 3  $\mu\text{m}$  (L-3) was different. Thus, instead of a surface coated with crystals, cells with a glassy appearance, some of which had a (black coloured) centre pore were observed, surrounded by white crystals. The cross-section exhibited no continuous layer of crystals at the surface, which explained the low gloss of the glaze, though the presence of crystals at a certain depth was observed.

Cell shape indicated that the crystals had moved from the tile surface owing to the excessive fusibility of the L-3 frit because of its smaller particle size **iError! No se encuentra el origen de la referencia.** This led the L-3 frit to melt before the underlying glaze did, and to penetrate through the voids between frit particles of the underlying glaze, forming the cells observed at the surface. These cells were, in fact, underlying glaze frit particles that had surfaced.

To confirm this assumption, fusion tests were performed of the underlying glaze and of lustre frits L-40 and L-3 in a hot stage microscope. The results (not included owing to space constraints) indicated that frit L-40 exhibited similar sintering and softening temperatures to those of the underlying glaze. However, after milling to 3  $\mu\text{m}$  (L-3), these temperatures decreased by about 80°C, which explained the above behaviour.

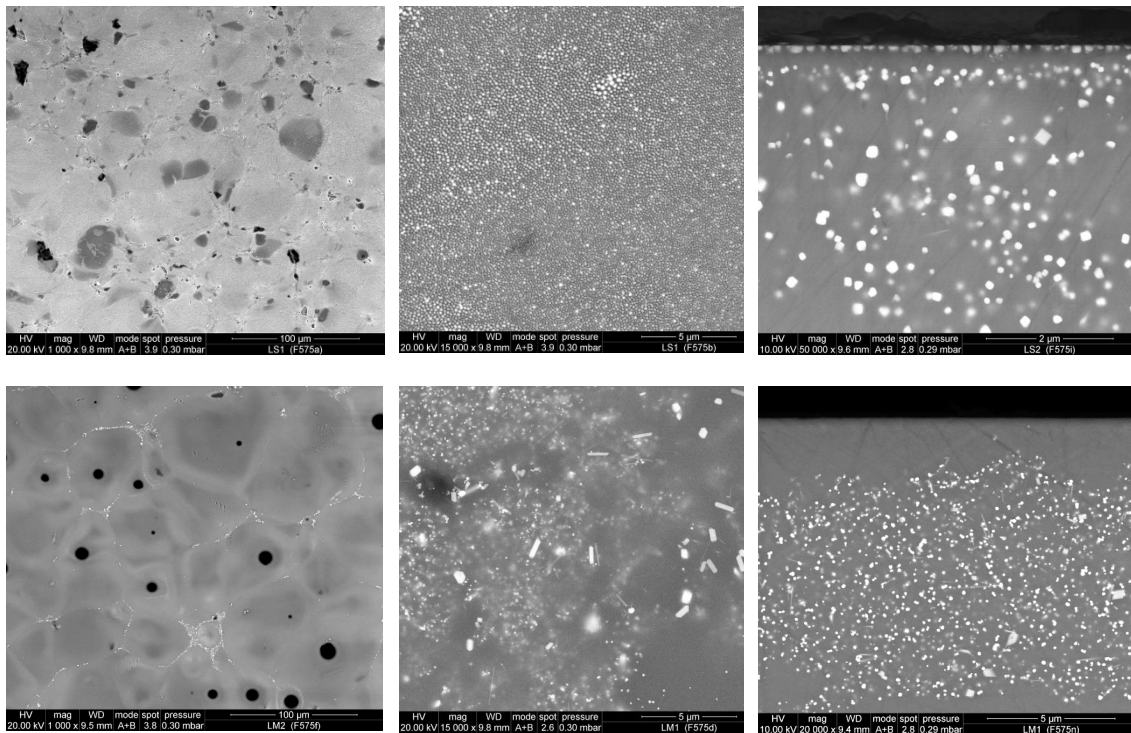
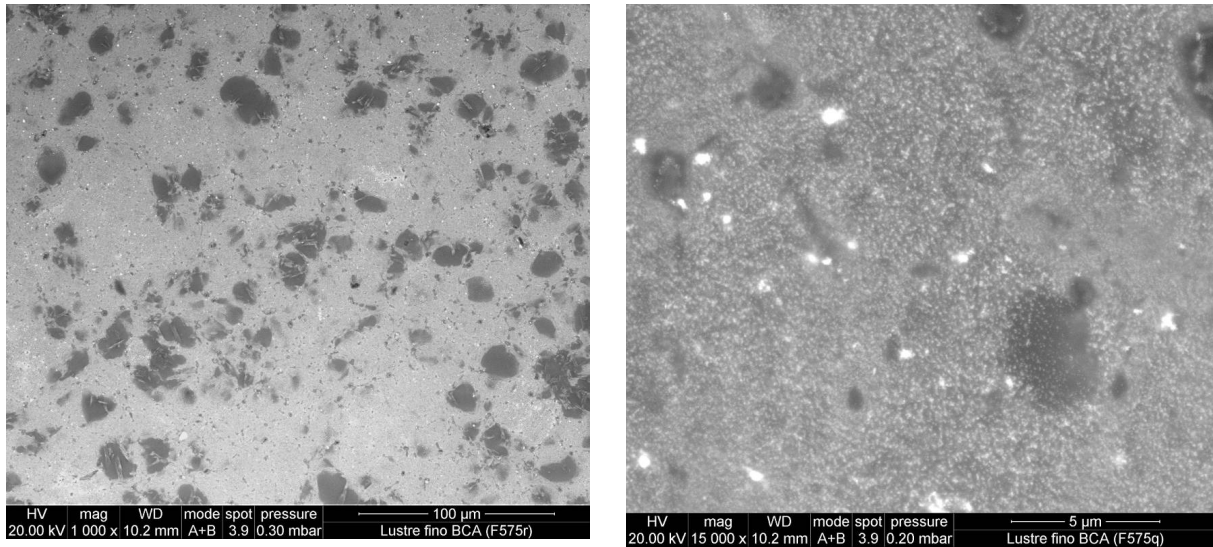


**Figure 1.** Surface appearance (left and centre) and cross-section (right) of tiles with frit L-40 (top) and L-3 (bottom) application observed by SEM.  $T=1120^{\circ}\text{C}$ .

### 3. INFLUENCE OF UNDERLYING GLAZE REFRACTORINESS

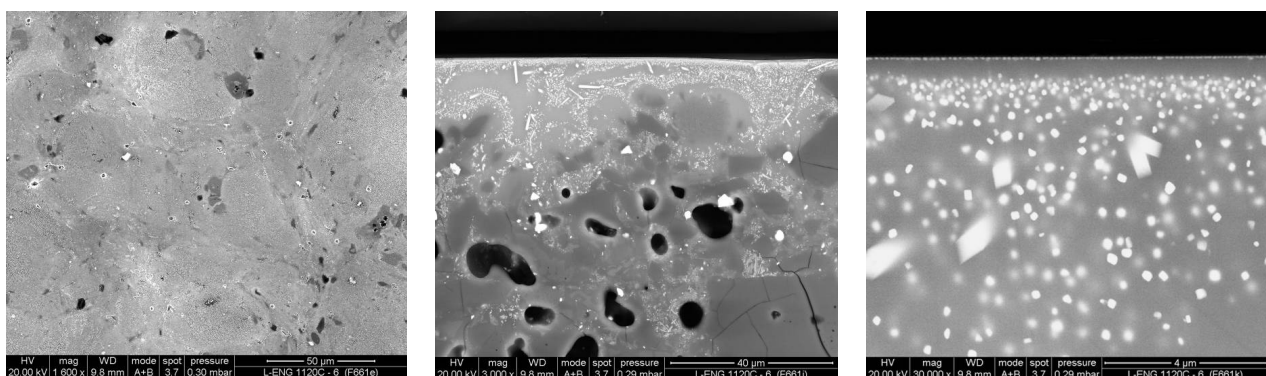
The results of the previous section suggested that the non-existence of a continuous surface layer of cerium oxide crystals was mainly due to a mismatch between the fusibility of the lustre frit and that of the underlying glaze. To confirm this, a tile with frit L-3 application on a fast double-fire glaze was fired at a  $100^{\circ}\text{C}$  lower temperature,  $1020^{\circ}\text{C}$  (L-3/1020). In addition, the L-3 frit was also applied onto an engobe at  $1120^{\circ}\text{C}$  (L-3/ENG), as an example of a substrate with greater melt viscosity.

Figure 2 shows the surface appearance of the tile fired at a lower temperature on a double-fire glaze. Comparison of this figure with that corresponding to the L-3 tile fired at  $1120^{\circ}\text{C}$  (Figure 1 bottom, left), reveals that lowering the firing temperature caused the crystal-free cells to disappear, the surface displaying a greater number of cerium oxide crystals than the L-3 tile. The appearance of this tile confirmed the excessive fusibility of the L-3 frit for firing at  $1120^{\circ}\text{C}$  on a single-fire transparent glaze, which led it to penetrate between the transparent glaze particles that had not yet melted. Nevertheless, there were still more (dark) crystal-free areas in the L-3/1020 sample than in the L-40 sample (Figure 1, top left). In addition, comparison at higher magnifications of the areas with cerium oxide crystals of the L-40 and L-3/1020 tiles indicates that, in the latter, the devitrified crystals were smaller, which could be due to the lower firing temperature used for this tile.



**Figure 2.** Surface appearance of the tile with frit L-3 (L-3/1020) application observed by SEM.  $T= 1020^{\circ}\text{C}$ .

The appearance of the tile with L-3 frit application on engobe, fired at  $1120^{\circ}\text{C}$ , is shown in Figure 3. Given the greater refractoriness of the engobe layer, absence of the lustre effect, owing to penetration of the L-3 frit through the voids in the unmelted engobe layer, might have been expected. However, though a certain penetration (centre image) may be noted, the tile surface is also observed to be made up of a continuous layer of cerium oxide crystals, resembling that resulting from the L-40 frit, which was responsible for the lustre effect on this tile. The reason for this behaviour is to be sought in the greater impermeability of the engobe layer (comprising 20% clay, 30% frit, and 50% other raw materials) in relation to that of the transparent glaze layer (comprising 95% frit and 5% kaolin), together with its greater melt viscosity, which also adversely affected cerium oxide crystal movement.



**Figure 3.** Surface appearance (left) and cross-section (centre and right) of the tile with L-3 frit application on the engobe observed by SEM.  $T=1120^{\circ}\text{C}$ .

## 4. INFLUENCE OF FRIT COMPOSITION

With a view to adapting lustre frit fusibility to the underlying glaze to prevent its penetration into the latter, a series of modifications in the starting lustre frit composition were performed, consisting of the progressive decrease in the amount of some fluxing oxides. The resulting composition was subsequently optimised, using the design of experiments technique, modifying the amounts of other oxides.

### 4.1. PRELIMINARY STUDY

The test compositions are detailed in Table 1. It shows that the changes performed consisted of reducing the boron oxide and alkali oxide content and raising the silica content. The other oxides were not modified.

| Oxides                         | L-3  | LR-1 | LR-3 | LR-4 |             |
|--------------------------------|------|------|------|------|-------------|
| SiO <sub>2</sub>               | ●●●● | ●●●● | ●●●● | ●●●● | ●: 0–5%     |
| Al <sub>2</sub> O <sub>3</sub> | ●●●  | ●●●  | ●●●  | ●●●  | ●●: 5–10%   |
| B <sub>2</sub> O <sub>3</sub>  | 6.4  | 4.4  | 4.4  | 3.0  | ●●●: 10–20% |
| CaO                            | ●●   | ●●   | ●●   | ●●   | ●●●●: >20%  |
| Na <sub>2</sub> O              | 2.0  | 1.0  | -    | -    |             |
| K <sub>2</sub> O               | 3.2  | 2.2  | -    | -    |             |
| ZrO <sub>2</sub>               | ●    | ●    | ●    | ●    |             |
| BaO                            | ●    | ●    | ●    | ●    |             |
| ZnO                            | ●●   | ●●   | ●●   | ●●   |             |
| CeO <sub>2</sub>               | ●●   | ●●   | ●●   | ●●   |             |

**Table 1.** Test frit compositions (% by weight).

The frits were obtained on laboratory scale by melting at 1500°C, followed by milling to a maximum size of 3 μm ( $d_{97}=3\mu\text{m}$ ). The applications were performed with a 20 g dry solids/m<sup>2</sup> laydown on a zirconium white glaze. Firing temperature was 1120°C. The surface appearance of the tiles observed by SEM is shown in Figure 4.

All tiles exhibited circular areas (cells) that contained no crystals, which led the resulting lustre effect to be less intense than that of the L-40 frit. Note that, as frit fluxes were eliminated, the crystal-occupied areas increased, resulting in higher gloss. Thus, while in the L-3 tile the crystal-free areas occupied almost the entire surface and it was difficult to observe the cells, these could be clearly observed in the LR-3 and LR-4 tiles, which were those in which all alkali oxides had been eliminated. This indicates that lustre frit penetration through the underlying glaze decreased owing to the increase in lustre frit melt viscosity, which must progressively approach that of the underlying glaze, leading to increased gloss (Table 2).

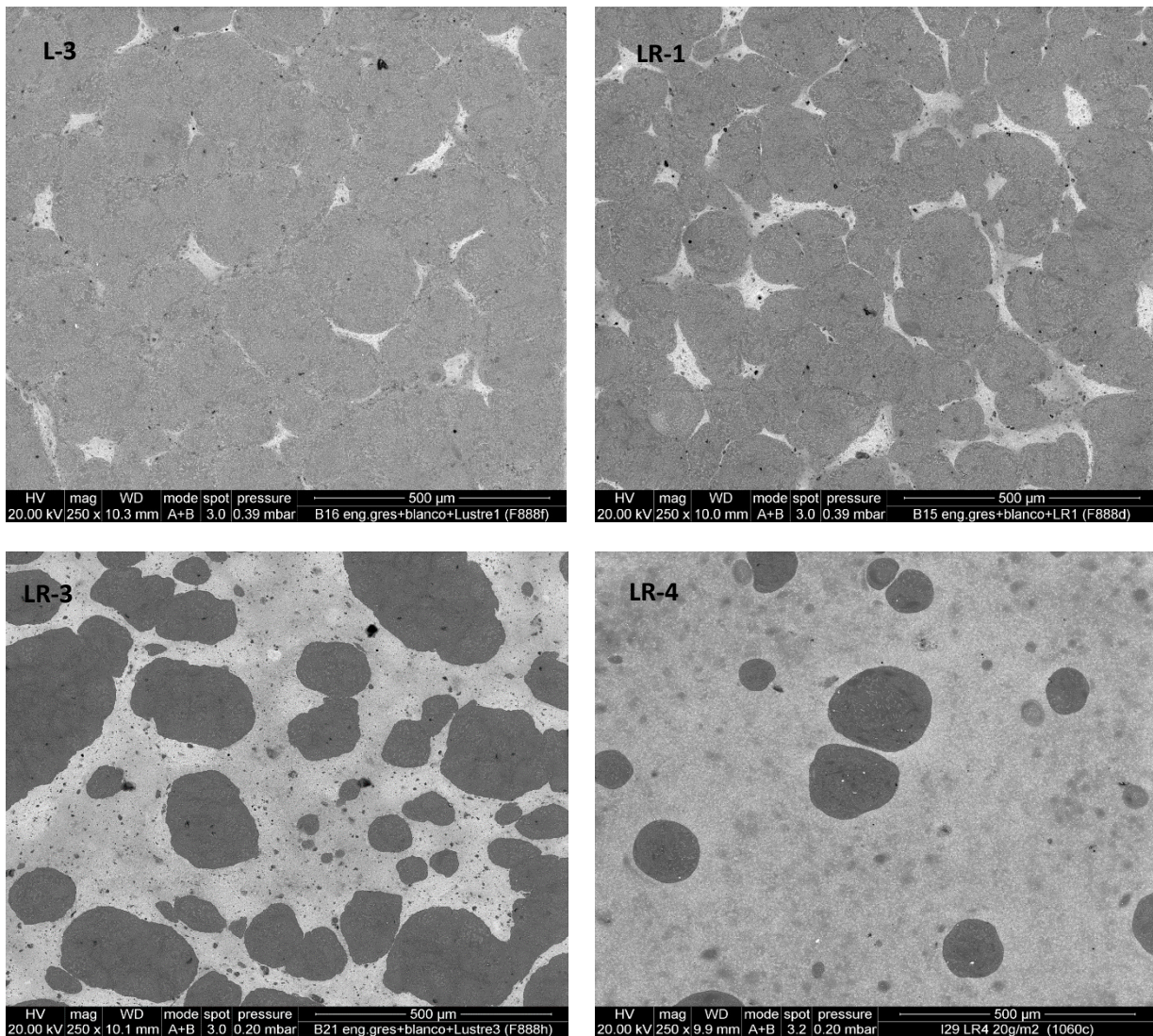


**Figure 4.** Surface appearance of the tiles with frit L-3, LR-1, LR-3, and LR-4 applications observed by SEM.  $T=1120^{\circ}\text{C}$ .

Figure 5 shows the cross-section of the tile with LR-4 frit. It shows the presence of a considerable number of crystals at the surface, which crystallised at what was initially the surface of the frit particles. This effect may be clearly noted in the top left and centre of the figure, in which crystal-free areas are observed, corresponding to the frit particle, delimited by these crystals. On the other hand, the presence of small cerium oxide crystals together with acicular zirconium silicate crystals indicates that there was a certain interaction between both layers, owing to partial penetration of the LR-4 frit in the underlying glaze.

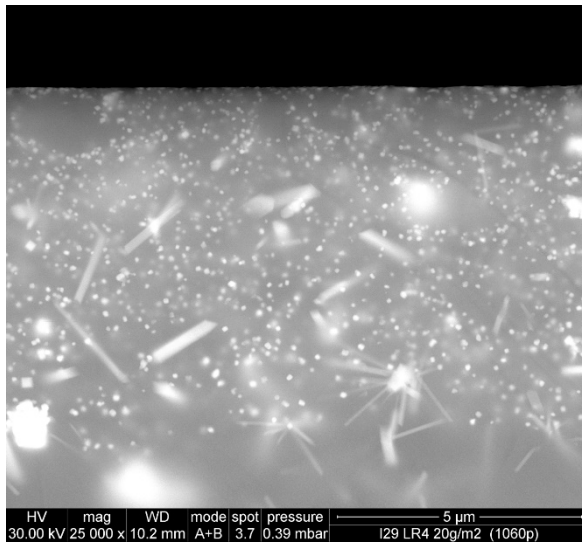


**Figure 5.** Appearance of the cross-section of the LR-4 tile observed by SEM.  $T=1120^{\circ}\text{C}$ .

| Frit | Gloss 60°C |
|------|------------|
| L-3  | 90         |
| LR-1 | 95         |
| LR-3 | 125        |
| LR-4 | 140        |

**Table 2.** Gloss values

As the devitrified crystals formed at what was initially the frit particle surface, when frit particle size was high ( $d_{97}=40\ \mu\text{m}$ ) practically all detected crystals were at the tile surface because below the crystal layer there was a crystal-free fringe of a thickness similar to that of frit particle size. In contrast, when the frit particles were small, the signal reaching the microscope detector came both from surface crystals and the crystals at a certain depth (sub-surface), owing to the absence of the crystal-free fringe as a result of the small size of the frit particles.

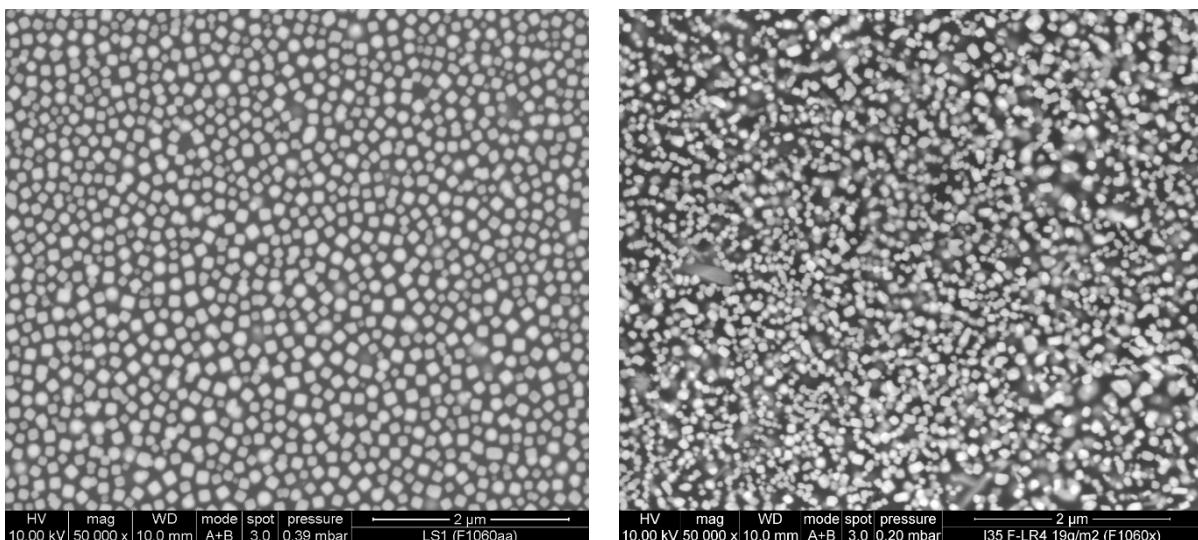


**Figure 6.** Surface appearance of tile with frit lustre application observed by SEM. L-40 (left) and LR-4 (right).  $T=1120^{\circ}\text{C}$ .

## 4.2. INFLUENCE OF THE AMOUNT OF APPLIED FRIT

This section examines the influence of the applied amount of lustre frit on the resulting gloss, for which different amounts of frits L-40 and LR-4 were applied onto an underlying glaze. After the tiles had been fired, the thickness of the lustre frit layer and the gloss were determined. The results are plotted in Figure 7. In this figure, the typical layer thickness of an inkjet application of effect ink (LR-4) was 7  $\mu\text{m}$ , whereas that of a screen print layer (L-40) was 25  $\mu\text{m}$ .

In both applications it was observed that, initially, there was a marked increase in gloss with thickness and that, from a certain thickness onwards, gloss stabilised. Under typical application conditions for each frit (inkjet printing for frit LR-4, 7  $\mu\text{m}$  thickness, and screen printing for frit L-40, 25  $\mu\text{m}$  thickness) the gloss provided by the LR-4 frit was lower than the gloss of frit L-40, due to the thinner inkjet printing layer. However, as the inkjet layer became thicker, gloss increased very quickly, exceeding that of the screen printing application.

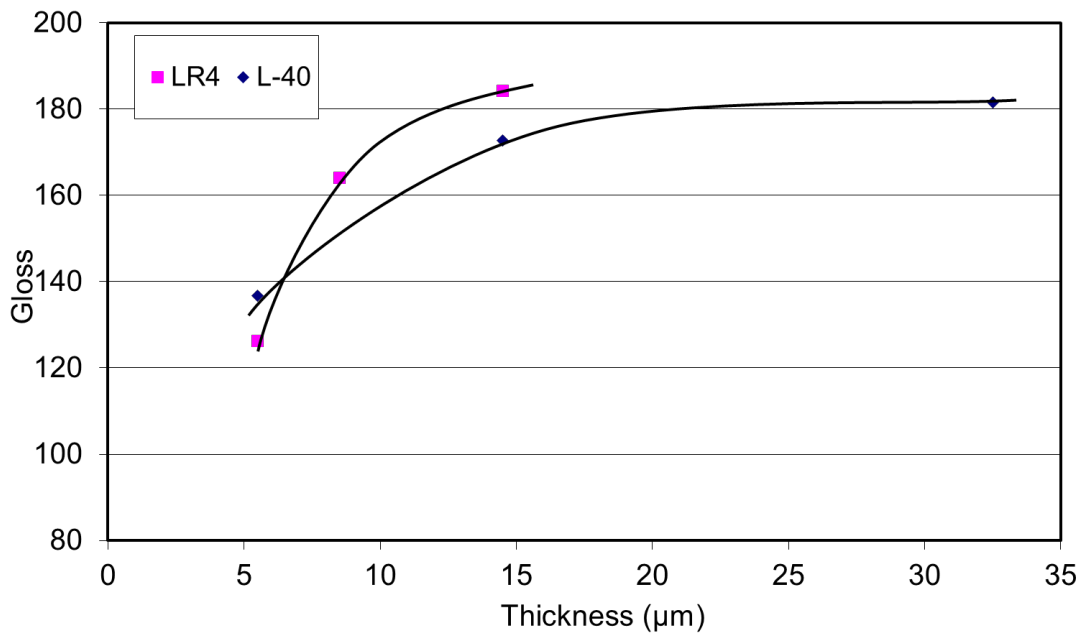


**Figure 7.** Variation of glazed surface gloss with layer thickness.

Figure 8 shows images of the tile surface with different amounts of frit. As was to be expected, as the amount of frit increased, the proportion of the area covered by crystals rose, which was consistent with the trend observed for gloss values. The crystals that devitrified from the L-40 frit were larger and had more defined edges than those of the LR-4 frit, but they were less numerous and occupied a smaller surface area.

The top centre image and the bottom right image correspond to the same layer thickness (15  $\mu\text{m}$ ) applied with each of the frits. It may be verified that, though the crystals provided by frit LR-4 were smaller, the surface area covered by the crystals was larger, which explains why the gloss obtained on using the LR-4 frit was higher than that of the L-40 frit at the same layer thickness.

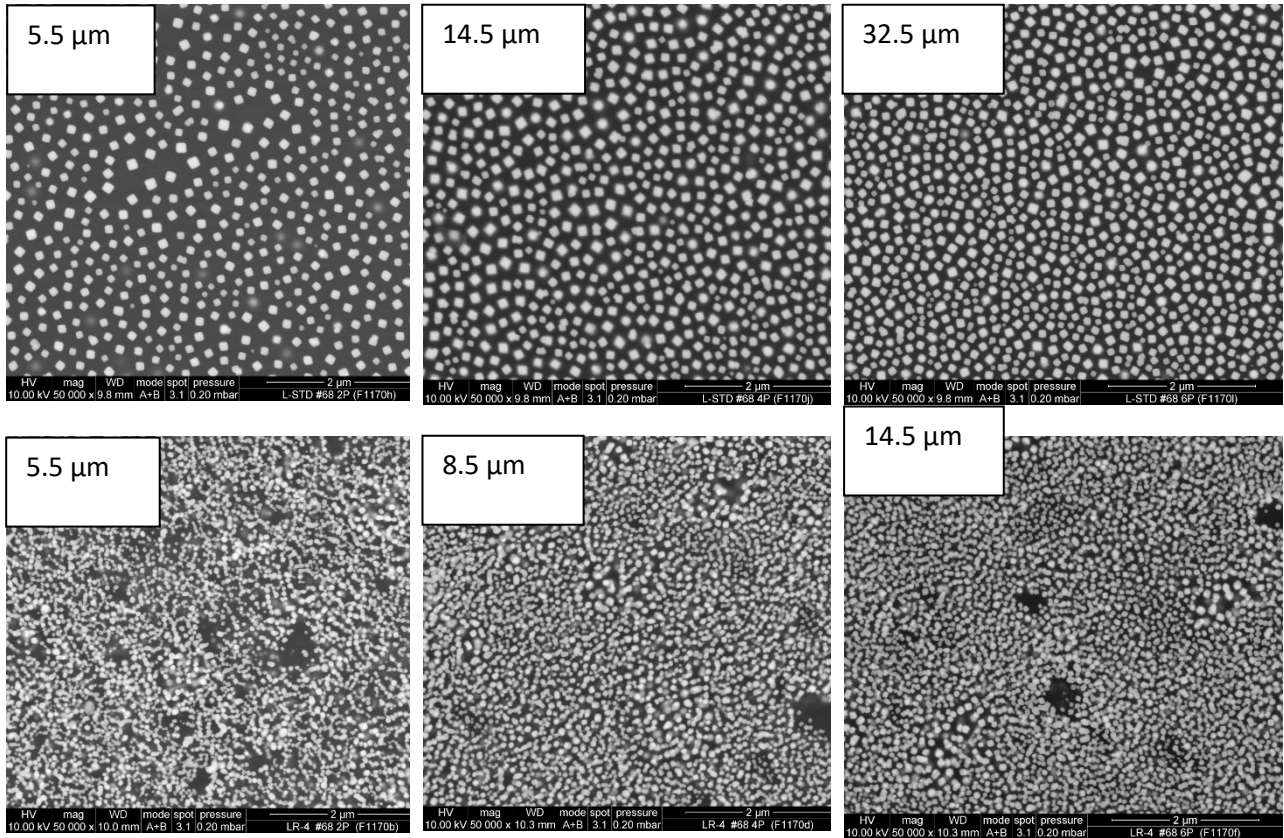


**Figure 8.** Surface appearance of tiles with applications of different amounts of lustre frit observed by SEM. L-40 (top) and LR-4 (bottom).  $T=1120^{\circ}\text{C}$ .

### 4.3. OPTIMISATION OF THE FRIT COMPOSITION

The reduction in the amount of some frit oxides in order to decrease frit fusibility and minimise frit penetration into the underlying glaze significantly improved gloss as a result of the decrease in surface area not occupied by cerium oxide crystals. However, the presence of circular areas without crystals, these moreover being crystals that were slightly smaller and not all at the tile surface, led the resulting gloss to be lower than required. Consequently, new compositions were prepared to optimize frit gloss, a mixture design software being used for this purpose and for the interpretation of the results.

Starting with composition LR-4, the following oxides were selected for study:  $\text{Al}_2\text{O}_3$ ,  $\text{CaO}$ ,  $\text{BaO}$ , and  $\text{ZnO}$ . The study variation range was  $\pm 3\%$  for all oxides, except for  $\text{BaO}$ , which was  $\pm 2\%$ .

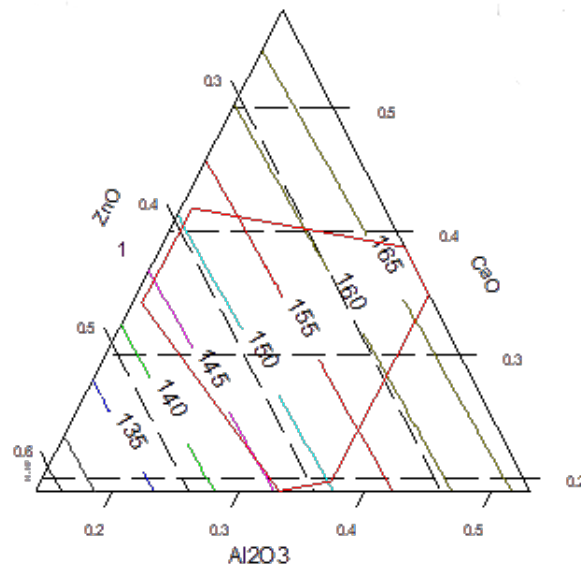
A linear variation of gloss ( $y$ ) with content in each of the frit oxides ( $x_1, x_2, \dots, x_n$ ) was assumed in the range considered, equations like the following being obtained:

$$y = a_0 + a_1x_1 + a_2x_2 + \dots + a_nx_n$$

where  $a_0, a_1, a_2, \dots, a_n$  are the coefficients that relate gloss to composition.

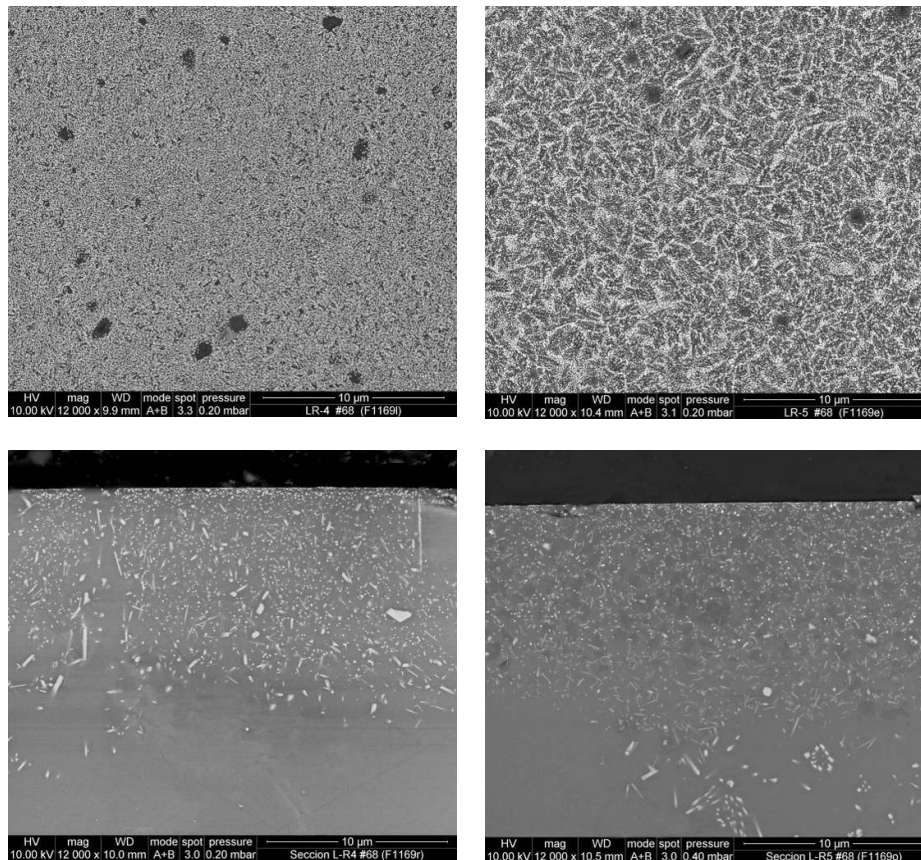
The results indicated that of the 4 oxides considered, the BaO did not have a significant effect on the gloss developed by the lustre frit, while Al<sub>2</sub>O<sub>3</sub> and CaO raised gloss and ZnO lowered gloss.

Figure 9 depicts a ternary diagram in which the BaO content was kept constant at the tested minimum value. Note that the ternary diagram axes were defined as a fraction of unity, so that the sum of the contents of the 4 studied oxides was unity. The lines represent compositions that gave rise to the same gloss value. The trend observed indicates that maximum gloss was reached on maximising, within the studied range, Al<sub>2</sub>O<sub>3</sub> and CaO content, and minimising ZnO content. Optimised composition (LR-OP) provided 25 more units of gloss than LR-4, reaching a gloss of 165 units. This value was 15 points below that of frit L-40, though it should be borne in mind that the amount of ink applied by inkjet printing and by screen printing was very different, which also gave rise to different layer thicknesses.



**Figure 9.** Evolution of gloss with frit composition.

Finally, the surface and cross-section of the tiles with the frit LR-4 and LR-OP applications were examined by SEM. The main difference was that, while the crystals in the LR-4 frit were uniformly distributed at the fired glaze surface, in the optimised frit, the crystals were concentrated around small areas, 1–3 μm long, which also contained crystals, forming a network delimiting what might have been starting frit particles. The same appearance was also observed in the tile cross-sections and could be due to greater crystallisation at the surface of the frit particles.



**Figure 10.** Surface appearance of tiles with LR-4 frit (left) and LR-OP (right) applications observed by SEM.  $T=1120^{\circ}\text{C}$ .

## 5. CONCLUSIONS

In this study, a frit composition was developed that devitrifies cerium oxide and zirconium to provide the lustre effect in conventional glazing lines as well as in “full digital” lines. The results indicate that frit milling to the sizes required for inkjet application excessively increased frit fusibility with respect to the underlying glaze, causing the frit, on melting, to penetrate through the voids between the (as yet unmelted) underlying glaze particles, keeping the continuous surface layer of crystals, which provides the high gloss, from forming.

Adjusting the fusibility of the lustre frit to that of the underlying glaze enabled the surface area occupied by the devitrified crystals to be increased. However, the smaller frit particle size, the fact that some crystals did not lie at the surface, and the low amount of frit applied by inkjet printing led to lower gloss than that of the lustre frits applied by screen printing or rotogravure.

For both inkjet and screen printing applications, it was verified that, as the applied amount of frit increased, the gloss value also rose as a result of the higher number of crystals at the surface. It was observed that, when the same layer thickness was applied, the developed lustre frit provided higher gloss than the conventional frit. This occurred because, though the devitrified crystals were smaller, the surface area occupied by these crystals was larger.

It was verified that, for the studied frit, the increased  $\text{Al}_2\text{O}_3$  and  $\text{CaO}$  content improved the resulting gloss, while  $\text{ZnO}$  reduced it. The frit provided a gloss value that

was 15 units lower than that of a conventional frit gloss, this being mainly due to the smaller applied amount of frit. Additional work is therefore required to optimise the developed frit composition and further enhance cerium oxide and zirconium crystal devitrification.

## 6. REFERENCES

- [1] Amorós, J.L.; Gozalbo, A.; Orts, M.J.; Belda, A.; Rodrigo, J.L.; Sanmiguel, F. Estudio de algunas de las variables que influyen sobre el brillo de vidriados obtenidos a partir de una mezcla de frit y oxido de wolframio. In: proceedings of the IIIrd World Congress on Ceramic Tile Quality. Castellón. Cámara de Comercio, Industria y Navegación. Vol.II, 47-59, 1994.
- [2] Gualtieri, A.F.; Canovi, L.; Viani, A.; Bertocchi, P.; Corradini, C.; Gualtieri, M.L.; Gazzadi, G.C.; Zapparoli, M.; Berthier, S. Mechanism of lustre formation in scheelite-based glazes. *Journal of the European Ceramic Society*, 33 (2013) 2055-2064.
- [3] Escardino, A.; Amorós, J.L.; Orts, M.J.; Mestre, S.; Belda, A.; Marco, J.; Salas, J.J. Estudio del efecto lustre en vidriados. In: Proceedings of the VIth World Congress on Ceramic Tile Quality. Castellón. Cámara Oficial de Comercio, Industria y Navegación. Vol.I, 93-109, 2000.
- [4] Siligardi, C.; Montecchi, M.; Montorsi, M.; Pasquali, L. Ceria-Containing Frit for Luster in Modern Ceramic Glaze. *Journal of the American Ceramic Society*, 93 (2010) 2545-2550.
- [5] Malins, J.P.; Tonge, K.H. Reduction processes in the formation of lustre glazed ceramics. *Thermochimica Acta*, 340-341 (1999) 395-405.
- [6] Manrique, J.; Usó, J.; Rubert, C.; Bou, E.; Garcia-Ten, F. J.; Morena A.; Pérez, M.R. Desarrollo de efectos estéticos mediante la aplicación de materiales submicrónicos. In: Proceedings of the XVth World Congress on Ceramic Tile Quality. Castellón. Cámara de Comercio, Industria